A Tale of Two Limits:
Fundamental Properties of Photonic-Crystal Fibers

Karen K. Lee, Ardavan Farjadpour, Yehuda Avniel, J. D. Joannopoulos, and
Steven G. Johnson[*]

Research Laboratory of Electronics, Massachusetts Institute of Technology,
77 Massachusetts Ave., Cambridge MA, USA

ABSTRACT

We present analytical results that shed new light on the properties of photonic-crystal fibers (optical fibers with periodic structures in their cladding). First, we discuss a general theorem, applicable to any periodic cladding structure, that gives rigorous conditions for the existence of cutoff-free guided modes—it lets you look at a structure, in most cases without calculation, and by inspection give a rigorous guarantee that index-guiding will occur. This theorem especially illuminates the long-wavelength limit, which has proved difficult to study numerically, to show that the index-guided modes in photonic-crystal fibers (like their step-index counterparts) need not have any theoretical cutoff for guidance. Second, we look in the opposite regime, that of very short wavelengths. As previously identified by other authors, there is a scalar approximation that becomes exact in this limit, even for very high contrast fibers. We show that this "scalar" limit has consequences for practical operation at finite wavelengths that do not seem to have been fully appreciated: it tells you when band gaps arise and between which bands, reveals the symmetry and "LP" degeneracies of the modes, and predicts the scaling of cladding-related losses (roughness, absorption, etc.) as the size of a hollow core is increased.

Keywords: photonic crystal, optical fiber, waveguide mode

1. INTRODUCTION

In this paper, we discuss some general analytical results for the properties of index-guided modes in a broad class of dielectric waveguides known as *photonic-crystal fibers*: waveguides surrounded by a *photonic crystal*[1] cladding that is periodic (at least asymptotically) in directions transverse to the waveguide axis.[2–4] Such fibers have been designed and fabricated to exhibit a number of remarkable properties compared to ordinary dielectric waveguides, from guiding light in hollow cores to extremely nonlinear solid-core fibers. The propagating modes of such waveguides (which typically involve complex high-contrast material geometries) can almost never be found analytically, nor do we suggest any analytical approximations here. Instead, we describe the results and derivation of general analytical theorems for such fibers, that illuminate their fundamental properties of index guidance, band gaps, cladding losses, and degenerate "LP" modes. The first result is a new theorem giving rigorous sufficient conditions for cutoff-free index-guided modes, and is especially informative in the long-wavelength limit (which is very difficult to study numerically) and for the design of single-polarization fibers. The second is an exploration of an old (but not widely known) theorem[5, 6] describing a rigorous scalar short-wavelength limit—we show that this limit leads to previously unappreciated consequences for the origin of the band gap in holey fibers, the (near) modal degeneracies, and the scaling of cladding-related losses as the core sizes is increased.

2. RIGOROUS CONDITIONS FOR CUTOFF-FREE INDEX-GUIDED MODES

The most common guiding mechanism in dielectric waveguides is *index guiding* (or "total internal reflection"), in which a higher-index *core* is surrounded by a lower-index cladding ε_c (ε is the relative permittivity, the square of the index). A schematic of several such dielectric waveguides is shown in Fig. 1. In particular, we suppose that the waveguide is described by a dielectric function $\varepsilon(x,y,z) = \varepsilon_c(x,y,z) + \Delta\varepsilon(x,y,z)$ such that:

[*]Corresponding author. E-mail: stevenj@math.mit.edu, Telephone: 617-253-4073.

(a) Cross section of a waveguide (e.g. a conventional fiber) with a homogeneous cladding and an arbitrary-shape core.

(b) Cross section of a photonic-crystal fiber with periodic cladding and arbitrary-shape core.

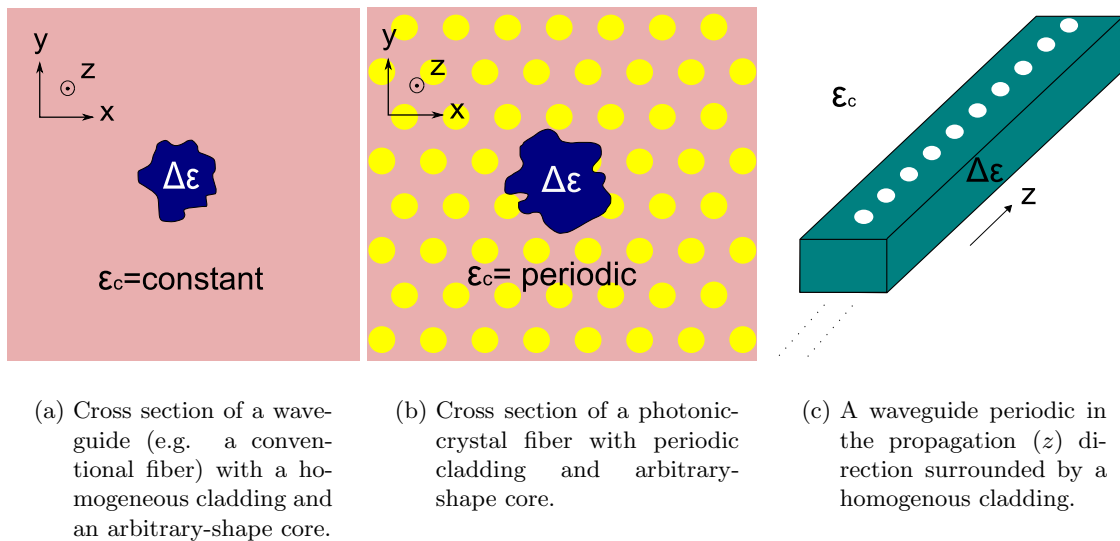(c) A waveguide periodic in the propagation (z) direction surrounded by a homogenous cladding.

Figure 1. Schematics of various types of index-guided dielectric waveguides. Light propagates in the z direction (along wich the structure is either uniform or periodic) and is confined in the xy direction by a higher-index core compared to the surrounding (homogeneous or periodic cladding).

ε, ε_c, and $\Delta\varepsilon$ are periodic in z (the propagation direction) with period a ($a \to 0$ for the common case of a waveguide with a constant cross-section); that the cladding dielectric function ε_c is either periodic in xy (e.g. in a photonic-crystal fiber) or homogeneous (e.g. in a conventional fiber); and the core is formed by a change $\Delta\varepsilon$ in some localized region of the xy plane, such that $\Delta\varepsilon \to 0$ as $|x^2 + y^2| \to \infty$. This includes a very wide variety of dielectric waveguides, from conventional fibers [Fig. 1(a)] to photonic-crystal "holey" fibers [Fig. 1(b)] to waveguides with a periodic "grating" along the propagation direction [Fig. 1(c)] such as fiber-Bragg gratings[7] and other periodic waveguides.[8,9] We exclude metallic structures (i.e, we require $\varepsilon > 0$), make the approximation of lossless materials (real ε), and for simplicity we consider only isotropic materials here; the case of substrates is considered below. Intuitively, if the refractive index is increased in the core, i.e. if $\Delta\varepsilon$ is non-negative, then we might expect to get exponentially localized index-guided modes, and this expectation is borne out by innumerable numerical calculations.[2–4]

However, an intuitive expectation of a guided mode is far from a rigorous guarantee, and upon closer inspection there arise a number of questions whose answers seem harder to guess with certainty. First, even if $\Delta\varepsilon$ is strictly non-negative, is there a guided mode at *every* wavelength, or is there the possibility of e.g. a long-wavelength cutoff (as some have suggested in holey fibers[10])? Second, what if $\Delta\varepsilon$ is *not* strictly non-negative, i.e. the core consists of partly increased and partly decreased index; it is known in such cases, e.g. in "W-profile fibers"[11] that there is the possibility of a long-wavelength cutoff for guidance, but precisely how much decreased-index regions does one need to have such a cutoff? Third, under some circumstances it is possible to obtain a single-polarization fiber, in which the waveguide is truly single-mode (as opposed to two degenerate polarizations in a cylindrical fiber)[12–17]—can this occur if only the core is asymmetrical, or is some further condition required? And when can one have single-polarization fibers with no long-wavelength cutoff (unlike most previous designs[12, 14–17])? It turns out that all of these questions can be rigorously answered for the very general geometries considered in Fig. 1, without resorting to approximations or numerical computations.

First, let us review the basic descriptions of the eigenmodes of a dielectric waveguide. In a waveguide as defined above, the solutions of Maxwell's equations (both guided and non-guided) can be written in the form of eigenmodes $\mathbf{H}(x,y,z)e^{i\beta z - \omega t}$ (via Bloch's theorem thanks to the periodicity in z),[1] where ω is the frequency, β is the propagation constant, and the magnetic-field envelope $\mathbf{H}(x,y,z)$ is periodic in z with period a (or is independent of z in the common case of a constant cross section, $a \to 0$). In the absence of the core (i.e. if $\Delta\varepsilon = 0$),

the (non-localized) modes propagating in the infinite cladding form the "light cone" of the structure;[2–4] and at each real β there is a fundamental (minimum-ω) space-filling mode at a frequency $\omega_c(\beta)$ with a corresponding field envelope $\mathbf{H}_c$.[2–4] Below the "light line" $\omega_c(\beta)$, the only solutions in the cladding are evanescent modes that decay exponentially in the transverse directions.[18] Therefore, once the core is introduced ($\Delta\varepsilon \neq 0$), any solutions with $\omega < \omega_c$ must be guided modes, since they are exponentially decaying in the cladding far from the core: these are the index-guided modes (if any).

2.1 The theorem

The theorem is then simple to state. Let $\mathbf{D}_c = \frac{1}{i\omega}(\nabla + i\beta\hat{\mathbf{z}}) \times \mathbf{H}_c$ denote the displacment-field envelope for the fundamental mode of the cladding. Then, there *must* be an index-guided mode at β if the following condition holds:

$$\int_{-\infty}^{\infty} dx \int_{-\infty}^{\infty} dy \int_0^a dz \left(\frac{1}{\varepsilon} - \frac{1}{\varepsilon_c}\right) |\mathbf{D}_c|^2 = \int_{-\infty}^{\infty} dx \int_{-\infty}^{\infty} dy \int_0^a dz \, \Delta(x, y, z) |\mathbf{D}_c|^2 < 0, \tag{1}$$

where we have defined $\Delta = 1/\varepsilon - 1/\varepsilon_c$ (which is negative wherever the index is increased). Furthermore, if Eq. (1) holds and the fundamental mode of the cladding is doubly degenerate (which happens whenever the cladding has sufficient symmetry, *regardless* of the asymmetry of the core), there must be at least *two* index-guided modes. There are two important special cases:

- In the common case where $\Delta\varepsilon \geq 0$ ($\Delta \leq 0$) everywhere (i.e. the core only increases the index relative to the cladding), there is always a guided mode, for every β, and hence there is no long-wavelength cutoff (contrary to previous suggestions,[10] as discussed below).

- In cases where the cladding is homogeneous [e.g. in Fig. 1(a) and (c)], the condition is simply $\int \Delta < 0$, which is independent of β (and hence implies two guided modes at every β if it holds). This result is a generalization of an earlier theorem for the case of ε_c constant and ε independent of z.[19, 20]

Note that these are *sufficient* conditions, not necessary conditions, for index-guided modes to exist. So, for example, Eq. (1) is violated in a W-profile fiber with $\int \Delta > 0$ and some increased-index regions,[11] but there can stil exist a guided mode (albeit with a long-wavelength cutoff). We are unaware of any cutoff-free dielectric waveguides in which Eq. (1) does not hold, however, and hence suggest that it may indeed be a *necessary* condition for *cutoff-free* index-guided modes; however, this is currently only an interesting conjecture, with no proof.

2.2 Outline of the proof

The proof employs the variational (minimax) theorem to find an upper bound on the lowest eigenfrequency ω—if this upper bound is below the light line $\omega_c(\beta)$, that guarantees the existence of a guided mode. A similar strategy was employed for homogeneous claddings,[19, 20] and our particular approach was inspired by a related technique used to prove the existence of bound modes for two-dimensional attractive potentials in quantum mechanics.[21] In this section, we outline the basic structure of the proof, and in particular the crucial choice of an appropriate trial function to bound the frequency; the algebraic details are treated more exhaustively by another manuscript currently in preparation.

The variational theorem arises because the eigenfrequencies ω satisfy a Hermitian eigenproblem $\hat{\Theta}_\beta \mathbf{H} = \frac{\omega^2}{c^2}\mathbf{H}$ for the operator $\hat{\Theta}_\beta \triangleq \nabla_\beta \times \frac{1}{\varepsilon}\nabla_\beta \times$, with $\nabla_\beta \triangleq \nabla + i\beta\hat{\mathbf{z}}$,[1] The theorem states that the smallest eigenfrequency $\omega_{\min}(\beta)$ for a given β minimizes the Rayleigh quotient $Q(\mathbf{H})$:

$$\frac{\omega_{\min}^2}{c^2} = \inf_{\nabla_\beta \cdot \mathbf{H} = 0} \frac{\int \mathbf{H}^* \cdot \hat{\Theta}_\beta \mathbf{H}}{\int \mathbf{H}^* \cdot \mathbf{H}} \triangleq \inf_{\nabla_\beta \cdot \mathbf{H} = 0} Q(\mathbf{H}), \tag{2}$$

where the integrals are over the xy plane and the unit cell in z. That means that, if we can find *any* divergence-free "trial function" $\mathbf{H}$ such that $Q(\mathbf{H}) < \omega_c(\beta)^2/c^2$, we are done: there must be a mode below the light line, and such a mode must be guided. The constraint that the trial function be divergence-free ($\nabla_\beta \cdot \mathbf{H} = 0$) is crucial, since there are non-divergenceless fields for which $Q(\mathbf{H}) = 0$ (and is not an upper bound for the eigenfrequencies).

The trial function must resemble a guided mode in order for $Q(\mathbf{H})$ to form a useful upper bound for the guided-mode frequencies. Since one expects the guided modes to be exponentially decaying far from the core, it might seem reasonable to choose a $\mathbf{H}$ proportional to $e^{-r/L}$ (where r is the radius) for some sufficiently large L. It turns out that such a trial function fails, however, in the sense that one cannot prove that $Q(\mathbf{H})$ falls below the light line without actually solving for the eigenvalue or a similarly impossible analytical task. A closely related difficulty was observed in the quantum-mechanical analogue, and in fact any function of the form $f(r/L)$ (exponential, Gaussian, etc.) fails in a similar way for two-dimensional confinement[21] (as opposed to one-dimensional confinenent, where such simple functions work well and the variational proof is commonly assigned as a homework problem). For this reason, the proof of 2d bound modes in quantum mechanics was initially developed by much more complicated methods,[22, 23] but eventually variational approaches were developed by at least two groups.[21, 24] In particular, it turned out to be sufficient to use a trial function that decayed proportional to $e^{-(r+1)^\alpha}$ for sufficiently small α,[21] and this is the technique we use here.

In the limit of no confinement ($\Delta \to 0$) the trial function should obviously tend to the fundamental mode $\mathbf{H}_c = \nabla_\beta \times \mathbf{A}_c$ (where $\mathbf{A}_c$ is a vector potential function). Therefore, combined with the above considerations, we chose a trial function:

$$\mathbf{H} = \nabla_\beta \times (\gamma \mathbf{A_c}) = \gamma \mathbf{H_c} + \nabla \gamma \times \mathbf{A_c} \tag{3}$$

where γ is the function $\gamma(x^2 + y^2 + 1)$ (similar to Ref. 21) defined by:

$$\gamma = \gamma(x^2 + y^2 + 1) = \gamma(r^2 + 1) = e^{1-(r^2+1)^\alpha}. \tag{4}$$

This is chosen so that $\lim_{\alpha \to 0} \gamma = 1$ (hence $\mathbf{H} \to \mathbf{H}_c$) and $\lim_{r \to \infty} \gamma = 0$, where $r^2 + 1$ is used to ensure that γ is twice differentiable at the origin. By construction, $\nabla_\beta \cdot \mathbf{H} = 0$.

The remaining proof is straightforward, in principle: one substitutes Eq. (3) into the Rayleigh quotient $Q(\mathbf{H})$ and then proves that, in the limit of sufficiently small α, Q goes below the light line $\omega_c(\beta)$ if Eq. (1) holds. This involves a sequence of carefully bounded integrals to establish their $\alpha \to 0$ limits, similar to Ref. 21. One does *not* need to know any explicit form for the cladding fundamental mode $\mathbf{H}_c$ or $\mathbf{A}_c$—it is sufficient to know that they are of bounded magnitudes, which follows from the fact that Bloch's theorem applies to the unperturbed cladding (which was assumed periodic). The algebraic details of this analysis are discussed in the longer manuscript mentioned above.

Furthermore, in many common cases, the fundamental mode $\mathbf{H}_c$ of the unperturbed cladding is doubly degenerate. This is the case whenever the cladding is sufficiently symmetric (so as to admit a two-dimensional irreducible representation[25]), e.g. for a homogeneous cladding (where $\mathbf{H}_c$ is simply the two orthogonal polarizations) or for a triangular lattice of circular holes (the traditional holey fiber). In that case, the two degenerate modes produce a two-dimensional subspace of trial functions (3), all of which have Q below the light line (since the derivation above was independent of the fundamental mode chosen). This implies[19] that there are at least *two* guided modes whenever condition (1) holds. These two guided modes need not be degenerate, if the core is asymmetrical (however, we are assuming isotropic materials here; for birefringent materials, Eq. (1) and hence the existence of guided modes can still depend on polarization[13]).

2.3 Waveguides with cutoffs

The above theorem implies that either the assumptions of the theorem or Eq. (1) must be violated in order to obtain a waveguide with a cutoff. It is instructive to examine a few important such cases.

One familiar waveguide with a cutoff is a "W-profile" fiber, in which an increased-index core is surrounded by a depressed-index annulus,[11] surrounded by a homogeneous cladding. The reason why this can have a cutoff is simple: in the fiber geometries analyzed to have a cutoff, the depressed-index region was large enough to make $\int \Delta > 0$.

There is at least one case in which one *desires* a cutoff: to obtain a waveguide which supports only a single polarization mode, the other polarization must be cutoff in some way. Two ways to achieve this have been proposed in the literature. Most commonly, one uses a waveguide in which Eq. (1) is violated entirely, so that *both* polarizations are cut off, but due to asymmetry one is cut off at a longer wavelength than the other.[12, 14–17]

Alternatively, one can use a birefringent core so that the core is only higher-index for one of the polarizations[13] (note that the equations in this manuscript are for isotropic materials only). However, the above analysis suggests a third way, one that does not seem to have been considered in the literature: one forms a structure in which the *cladding* is periodic but asymmetric (e.g. a triangular lattice of elliptical holes). In this case the theorem only guarantees a single guided mode for an increased-index core, and it should be possible to obtain a single mode with no cutoff, with a cutoff for the other polarization.

Another waveguide with a cutoff is any waveguide sitting on a substrate, for example a Silicon strip or ridge waveguide on an oxide substrate.[26] This violates the assumptions of our theorem because the cladding is not periodic, it is a step function (oxide below and air above). More revealingly, one could inquire where in our derivation we relied on the periodic property that now fails—the answer, interestingly enough, is the assumption of that a fundamental mode of the cladding *exists*. In step-function cladding, the light line is simply the light line of the oxide, but there is no eigenmode at this frequency (such an eigenmode would have to be a constant in the oxide and non-constant in the air, and it is then impossible to satisfy the boundary conditions). Put more formally, our key assumption was not so much that the cladding is periodic, but that the infimum of the cladding spectrum at each β is itself an eigenvalue, which is true for periodic claddings where Bloch's theorem holds, but perhaps also for other cases.

Finally, some numerical evidence has been proposed for the claim that a holey fiber with a solid (filled-hole) core has a long-wavelength cutoff,[10] which would seem to contradict our theorem since $\Delta \leq 0$ in that case. This evidence, however, seems to be an artifact of the finite computational cell size. As the wavelength is increased (β is decreased), there should always be a guided mode in such a structure, but the modal diameter will increase rapidly with wavelength. In a simulation with absorbing boundary conditions (or an experiment), the mode will seem to be "cut off" when the modal diameter exceeds the diameter of the fiber used. Moreover, there is reason to believe that the modal diameter increases *exponentially* fast with the wavelength, which is why numerical study of the long-wavelength limit is so difficult. In quantum mechanics (scalar waves) with a potential well of depth V, the decay length of the bound mode increases as $e^{C/V}$ when $V \to 0$, for some constant C.[21,22] In electromagnetism, for the long wavelength limit, a homogenized effective-medium description of the structure becomes applicable,[27] and in this limit the modes are described by a scalar wave equation with a "potential" $-\omega^2\Delta\varepsilon$,[28] and hence the quantum analysis applies. Thus, by this informal argument we would expect the modal diameter to expand proportional to $e^{C\lambda^2}$ for some constant C (where $\lambda = 2\pi c/\omega$ is the vacuum wavelength). It is important to emphasize, however, that (as far as we are aware) there is no difference in this regard between photonic-crystal and conventional step-index fibers—for cutoff-free modes in both cases, the modal diameter will expand rapidly in the long-wavelength limit.

3. CONSEQUENCES OF THE SHORT-WAVELENGTH LIMIT

In this section, we now turn to results in an opposite regime—not about long-wavelength cutoffs but rather about short-wavelength limits. It is well known that, for low index contrasts, Maxwell's equations reduce approximately to a scalar wave equation,[28] which greatly simplifies the analysis of low-contrast step-index fibers.[29] Perhaps not so well known is the fact that a scalar-wave equation can also be used to rigorously and accurately describe *high*-contrast structures such as holey fibers—in particular, the scalar description becomes accurate (regardless of index contrast) in the *short-wavelength* limit. This short-wavelength scalar limit, derived rigorously in Ref. 5, was used by Birks et al. to predict the possibility of "endlessly single-mode" photonic-crystal fibers.[6] However, it has many other interesting consequences for photonic-crystal fibers (even for wavelengths that are not terribly small) that do not seem to have been fully explored, and which we discuss in the following sections. Moreover, we explain that a similar theorem applies for large-core hollow-core photonic-crystal fibers, which has important implications for the reduction of cladding-related losses.

We will consider three classes of photonic-crystal fiber, as depicted in Fig. 2: hollow-core fibers with (a) one-dimensionally periodic claddings (Bragg fibers) or (b) two-dimensionally periodic claddings of air holes (holey fibers); and (c) solid-core holey fibers. These xy cross-sections are assumed to be invariant in the axial (z) direction.
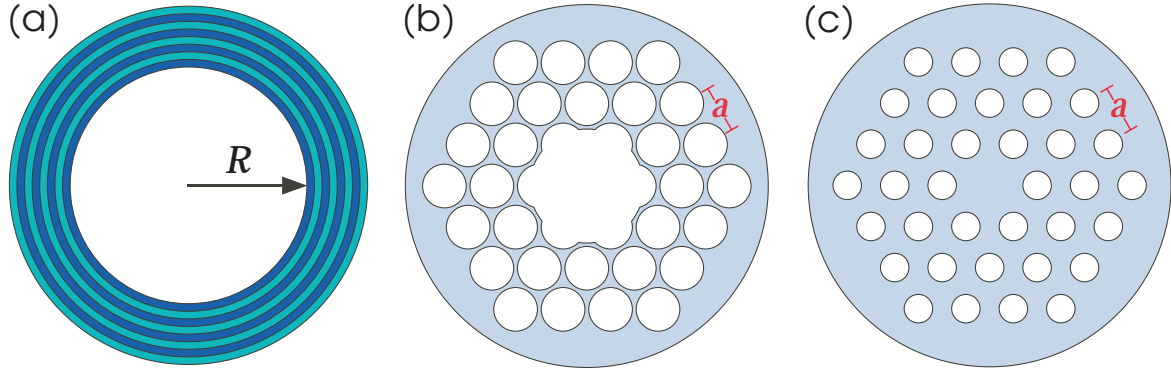
Figure 2. Three examples of photonic-crystal fibers. (a) Bragg fiber, with a one-dimensionally periodic cladding of concentric layers. (b) Two-dimensionally periodic structure (a triangular lattice of air holes, or "holey fiber"), confining light in a hollow core by a band gap. (c) Holey fiber that confines light in a solid core by index guiding.

3.1 The scalar limit

Consider first a solid-core holey fiber as in Fig. 2(c), and let us give an informal description of how the scalar limit arises. The key fact is that, in the short-wavelength limit, ray-optics becomes valid, and the light is totally internally reflected within the higher-index regions. Since almost all of the light is then within a homogeneous-index region, the low-contrast scalar description becomes valid. That is, the transverse field components are proportional to a scalar wave function $\psi(x,y)e^{i\beta z}$ described by a Schrödinger-like equation:

$$-\nabla_t^2\psi = k_t^2\psi, \tag{5}$$

where ∇_t denotes the transverse (x and y) components of ∇, and k_t is a *transverse wave number* defined as

$$k_t \triangleq \sqrt{\frac{\omega^2}{c^2}\varepsilon_{\text{hi}} - \beta^2}. \tag{6}$$

The influence of the air holes (or any lower-index region) appears only as a boundary condition on ψ: because of total internal reflection, $\psi = 0$ in the low-index regions.[5,6]

The corresponding vector-field solutions of Maxwell's equations are just $\psi\hat{x}$ and $\psi\hat{y}$. That is, in the short-wavelength scalar limit one obtains purely linearly polarized (LP) modes, and each scalar mode gives rise to *two* orthogonal vector modes. (The case of degenerate scalar fields is considered below.) Moreover, the field pattern of a given mode is then asymptotically *constant* (independent of frequency).

Mathematically, Eq. (5) with $\psi = 0$ in the air holes is exactly equivalent to the equation of a two-dimensional air/metal system: the equation for the TM ($\mathbf{E} \parallel \hat{z}$) electric field in air with perfect-metal rods replacing the low-index fiber regions. (Such a TM metallic structure is also described by a scalar wave equation with zero boundary conditions at the metal.) In this equivalence, ψ is replaced by E_z and k_t is replaced by ω/c. This equivalence means that one can use standard electromagnetic simulation techniques such as FDTD[30] to analyze the scalar limit, and one can also exploit existing understanding of 2d metallodielectric photonic crystals.[31]

In particular, consider the infinite defect-free cladding of a holey fiber, which is equivalent in the scalar limit to a triangular lattice of metal rods in air. The band diagram of the latter structure was computed using freely available FDTD software[32] and is plotted in Fig. 3. It shows the characteristic features of such a metallo-dielectric structure: a band gap from zero frequency up to some minimum frequency for light to fit between the rods, and another band gap between bands 2 and 3. When the fiber core is introduced (filling in an air hole, equivalent to removing a metal rod in the scalar limit), this defect introduces localized states in the core.[1] However, because the band gap is finite, there are only a finite number of modes localized.

In contrast, for a traditional step index fiber, the scalar limit corresponds simply to a circular core completely surrounded by hard walls, which supports an infinite number of localized modes (corresponding to the roots of various Bessel functions).[29] Thus, a holey fiber has a unique feature: it asymptotically supports only a finite
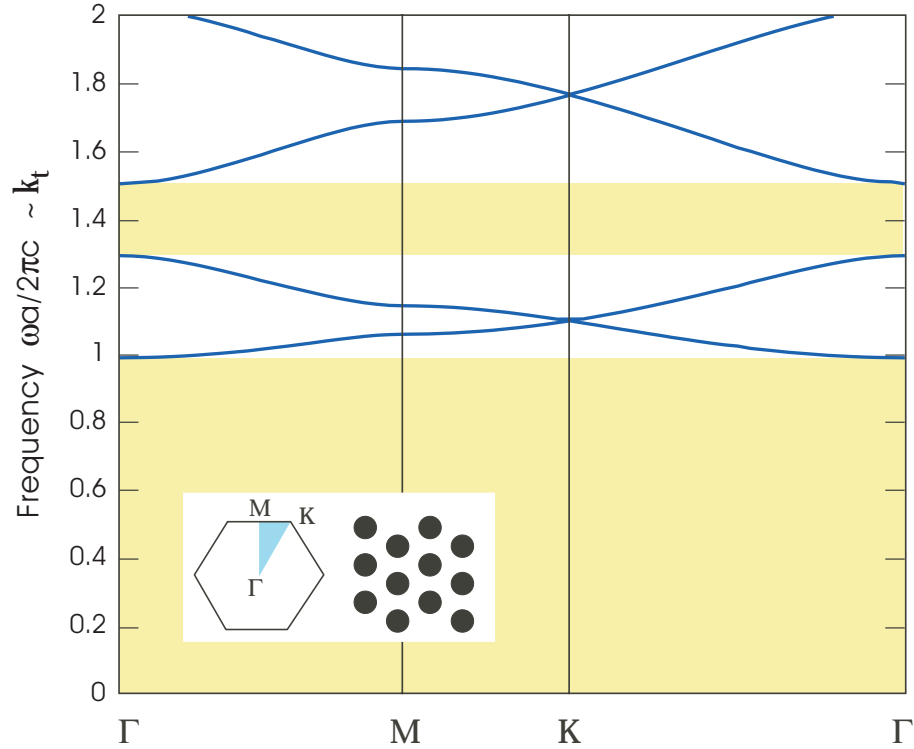
Figure 3. Band diagram for TM-polarized modes of a two-dimensional triangular lattice (period a) of perfect-metal cylinders (radius $0.3a$). Two band gaps are shown (shaded yellow), where the lowest band has a low-frequency cutoff characteristic of metallic structures. These bands are equivalent to the modes of the holey fiber in the scalar (large β) limit.

number of modes. Moreover, Birks et al. pointed out that, if the structure is chosen so that there is only a single mode in the scalar limit, then the waveguide will be "endlessly single mode".[6] This is not the only interesting consequence of the scalar limit, however.

3.2 LP modes

In the ordinary scalar approximation for low-contrast fibers, it is well known that one obtains LP modes: (approximately) linearly polarized field patterns, with two or four vectorial modes sharing the same intensity pattern and the same dispersion relation.[29, 33] A similar phenomenon occurs for holey fiber modes, and the phenomenon can be analyzed easily with the help of the scalar limit and group representation theory. In particular, consider the band diagram of a silica holey fiber, computed with a planewave method,[34] shown in Fig. 4. This fiber is endlessly *four*-mode: it has one doubly degenerate fundamental mode, and one doubly-degenerate mode higher-order mode whose dispersion relation lies nearly on top of those of two singly-degenerate moes. Why does this strange near-fourfold degeneracy arise?

This structure has sixfold symmetry, described by the C_{6v} symmetry group.[25] That group has four one-dimensional irreducible representations and two two-dimensional irreducible representations, which means that (excluding accidental degeneracies), the eigenmodes are expected to either be doubly degenerate or nondegenerate.[25] Exactly the same symmetry applies to the scalar Eq. (5) in the short-wavelength limit, so the scalar eigenfunctions ψ should either be nondegenerate or doubly degenerate.

Consider what this means for the vectorial solutions in the scalar limit. If ψ is non-degenerate, there will be doubly-degenerate vector modes $\psi\hat{\mathbf{x}}$ and $\psi\hat{\mathbf{y}}$. If ψ is doubly degenerate, however, that means there are two scalar solutions ψ_1 and ψ_2 with the same eigenvalue, and hence there will be *four* vector modes $\psi_{1,2}\hat{\mathbf{x}}$ and $\psi_{1,2}\hat{\mathbf{y}}$. That is, in the short-wavelength limit, we should expect to see pairs and quartets of modes lying on nearly on top
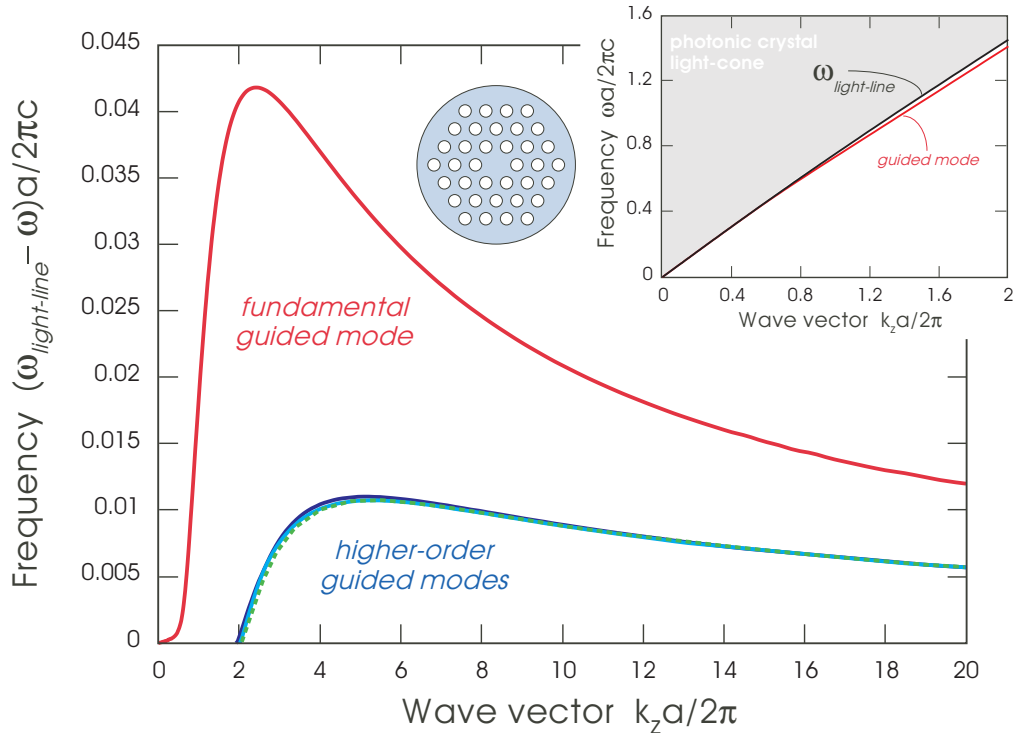
Figure 4. Band diagram of solid-core holey fiber (period a, hole radius $0.3a$, $\varepsilon = 2.1$ material corresponding to silica) as a function of axial wave vector k_z. The usual ω plot is inset, but for clarity we also plot the $\Delta\omega$ between the guided bands and the light line. The higher-order guided modes are three bands that are nearly on top of one another.

of one another, despite the fact that the symmetry should ostensibly only support double degeneracies. From Fig. 4, we see that this prediction of the scalar limit becomes rapidly accurate even for very moderate frequencies.

Moreover, the peculiar combinations of either one doubly degenerate mode or two nondegenerate modes and one doubly degenerate mode, seen in Fig. 4, turn out to be unavoidable consequences of symmetry. Products of two functions like $\psi\hat{\mathbf{x}}$ are described by *product representation theory*:[25] given a function ψ that falls into one irreducible representation of the symmetry group, and given a function $\hat{\mathbf{x}}$ that falls into another representation (one of the doubly degenerate representations of C_{6v}), their product *must* be composed of modes corresponding to certain representations/degeneracies.[25] In particular, for the C_{6v} symmetry group, if ψ is in one of the nondegenerate representations, the product $\psi\hat{\mathbf{x}}$ must be a doubly degenerate vector mode. And if if ψ is in one of the two-dimensional (doubly degenerate) representations, then $\psi\hat{\mathbf{x}}$ must consist of one doubly degenerate mode and two nondegenerate vector modes. Of course, if one has a different symmetry group, the possible degeneracies will be different, but the key point is that the exact combinations of vector mode symmetries and near-degeneracies that appear at short wavelengths can be exactly predicted from group theory and the short-wavelength scalar limit.

3.3 The origin of the holey-fiber bandgap

Instead of confining light in a solid core by traditional index-guiding, a photonic-crystal fiber can guide light in a *hollow* core by using a photonic bandgap.[2–4] Such a photonic bandgap is shown in Fig. 5, which plots the light cone of the infinite (no core) cladding of a holey silica fiber computed by a planewave method.[34] The gaps of such a fiber form characteristic "fingers" extending into the light cone from the right.[2–4] Moreover, the first (fundamental) gap of the triangular-lattice holey fiber is between the fourth and fifth bands (as discussed below). As it turns out, the scalar limit provides a simple, rigorous explanation of why these gaps arise, and why specifically between the fourth and fifth bands.
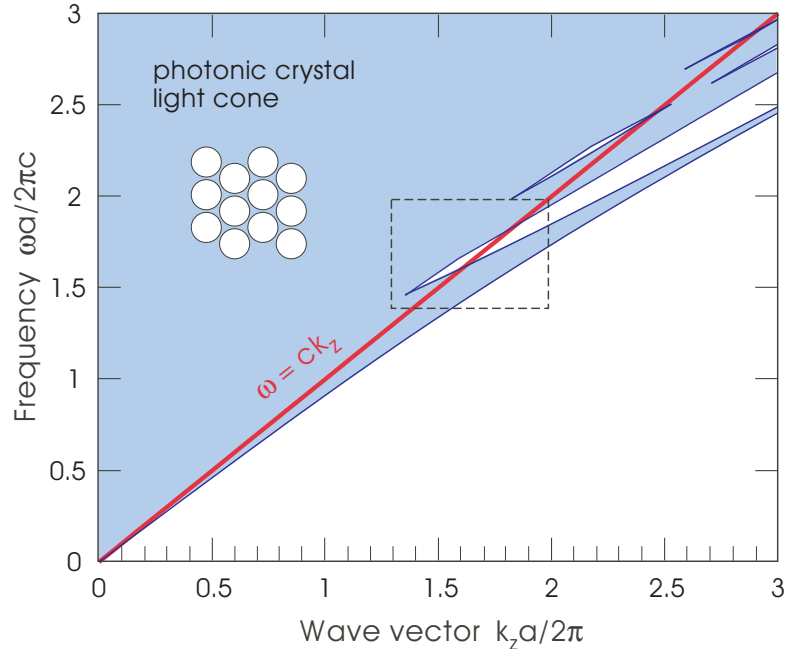
Figure 5. Projected band diagram, as a function of out-of-plane wave vector k_z, for a triangular lattice of air holes (inset: period a, radius $0.47a$) in $\varepsilon = 2.1$. This forms the light cone of the holey fiber from Fig. 2(b), with gaps appearing as open regions. The light line of air, $\omega = ck_z$, is shown in red.

First, we should emphasize that the band gaps in such a holey fiber are *not* a consequence of the two-dimensional photonic band gaps that arise for a lattice of air holes in dielectric.[1] Those gaps correspond to $\beta = k_z = 0$ (propagation purely in the xy plane); in order to be useful in a waveguide, the gaps must extend over a range of nonzero k_z. If the crystal has a *complete* (overlapping TE and TM) gap at $k_z = 0$, then indeed there will be a range of values of $k_z \neq 0$ over which the gap will persist (much like the gap in a Bragg fiber[35]). But the silica/air dielectric contrast of 2.1:1 is not sufficient to obtain such a complete two-dimensional gap (at least, not for these simple periodic geometries). The silica/air structure can have a TE gap, but not an overlapping TM gap, and for $k_z \neq 0$ both the TE/TM distinction—which was based on the $z = 0$ mirror symmetry plane for $k_z = 0$—and the gap disappear.

Rather than $k_z = 0$, the holey-fiber "finger" gaps arise from the $k_z \to \infty$ short-wavelength limit. This might obviously be guessed from the fact that the gaps open up from the right in the numerical results, but it can be predicted analytically. In particular, in the scalar limit we have the band diagram of Fig. 3, mathematically corresponding to a 2d metallo-dielectric photonic crystal, and this band diagram exhibits a gap between bands two and three (as well as higher-order gaps). This gap *must* open up for large enough k_z, as the scalar limit becomes accurate. Moreover, it must open *regardless of the index contrast*, and indeed band gaps have been observed experimentally for index contrasts as low as 1%.[36] As k_z is decreased towards zero, the scalar approximation becomes less and less accurate, and hence the gaps eventually close. This is why the gaps in photonic-crystal fibers most common form "fingers" that open monotonically as k_z is increased.

(Although this gap from the scalar limit opens regardless of index contrast, that is not sufficient for guiding light in an air core. One must also have a gap that extends above the light line of air, as shown by the dashed region in Fig. 5, in order to have guided modes that are not evanescent in air.[2–4])

Furthermore, the gap in the scalar limit was between the first and second scalar bands of Fig. 3. As discussed in the previous section, each scalar band corresponds to *two* vectorial modes, so therefore we expect the gap to open between the fourth and fifth vectorial eigenmodes of the cladding. This can be seen in the exact vectorial band diagram for the $r = 0.47a$ holey fiber at a particular $k_z a/2\pi = 1.7$, shown in Fig. 6. There is, of course, a gap below the first band, corresponding to the index-guided region below the light cone, and the next gap is
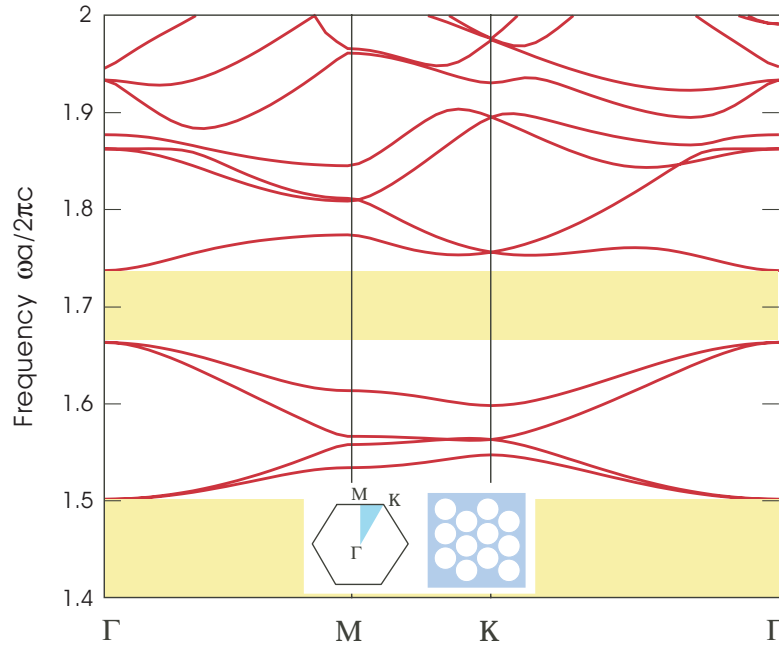
Figure 6. Band diagram versus in-plane wave vector in the irreducible Brillouin zone (inset) for the triangular lattice of air holes from Fig. 5, at an out-of-plane wave vector $k_z a/2\pi = 1.7$. Gaps are shaded yellow: the lower gap corresponds to the index-guiding region, and the upper gap corresponds to one of the band gaps inside the light cone where guiding in an air core is possible.

after the fourth band. Even the shape of the first four bands is reminiscent of the scalar band diagram from Fig. 3, where each of the scalar bands has been split into two vectorial bands.

3.4 Cladding losses in hollow-core fibers

Given a bandgap that extends above the light line of air, one can confine light in an air core; this can be done with either a holey fiber as in Fig. 2(b),[2–4] or via a Bragg fiber as in Fig. 2(a).[35] This is interesting and important for a variety of applications,[2] for example to operate fibers at wavelengths for which there is no transparent solid material.[37] In this case, a major source of loss in the fibers is associated with the cladding: the small exponential field tail penetrating into the cladding will lead to material-absorption losses, will leak through the finite number of layers of the crystal, and will be scattered by surface roughnesss at material interfaces.[35,38] One strategy to counteract such cladding-based losses is to increase the diameter of the air core,[35] which means that a smaller fraction of the air-guided mode will reside in the cladding. Unfortunately, increasing the core diameter leads to other problems, such as increased bending losses and other inter-modal coupling,[35] very similar to the tradeoffs that were faced decades ago in designing low-loss microwave transmission tubes (where the fields in the cladding gave Ohmic losses),[39] and so it is desirable to increase the core diameter as little as possible. Here, we give a general argument, based on the scalar limit, that the cladding-related losses should (asymptotically) scale inversely with the *cube* of the core diameter, similar to the well-known result for metallic tubes,[39] and demonstrate this scaling with numerical results.

All cladding-based losses in a dielectric waveguide scale with the fraction of the electric-field energy in the cladding. Material absorption losses, in fact, can be shown from perturbation theory to be exactly equal to the fraction of $\int \varepsilon |\mathbf{E}|^2$ residing in the cladding material, multiplied by a constant factor proportional the material's extinction coefficient and divided by the mode's group velocity.[35,40] The precise analysis of surface-roughness losses is complicated,[41] but nevertheless is proportional to the mean $|\mathbf{E}|^2$ at the surfaces (with a complicated proportionality factor depending on the roughness shapes and correlations[41]) and hence also scales as the fraction of the field energy in the cladding.[35] The field leakage through the finite number of crystal layers can easily be reduced exponentially by adding more layers,[1,35] so it is less of a concern, but it too scales with the squared
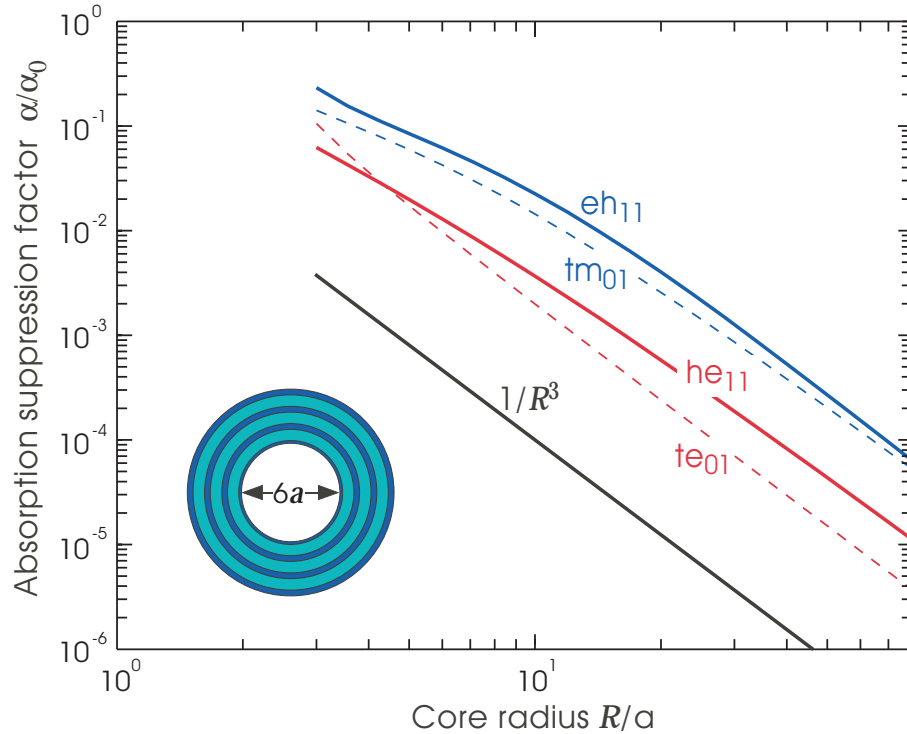
Figure 7. Scaling of the absorption suppression factor α/α_0 versus core radius R, at the quarter-wave frequency, for several modes of the hollow-core Bragg fiber with indices 2.7/1.6 (blue/green in inset). The absorption loss is assumed to be dominated by that of the low-index material. All modes asymptote to a $1/R^3$ scaling (shown as a black line, for reference).

field amplitude in the cladding.[35] Therefore it is sufficient to consider the scaling of the absorption loss, or of the fraction of field energy in the cladding, with the air-core radius R.

For example, let us consider a Bragg fiber, as depicted schematically in Fig. 2(a). Similar to a recent experimental fiber,[37] we suppose the concentric layers are made of a low-index polymer ($n = 1.6$) and a high-index chalcogenide glass ($n = 2.7$), arranged in a glancing-angle quarter-wave stack,[35] with the innermost layer being half of a polymer layer (a side-effect of the fabrication process, which happens to remove a troublesome surface state). Similar to the experimental structure, we assume that most of the absorption is due to the polymer, and we can then compute a dimensionless *absorption suppression* factor: the mode's absorption rate α divided by the absorption loss α_0 it would have propagating through the bulk polymer; this ratio is equal to the fraction of the electric-field energy in the polymer.[35] For various polarizations and modes of the fiber (labelled as described in Ref. 35), the numerically computed losses all are observed in Fig. 7 (computed using a transfer-matrix method[35]) to scale asymptotically as $1/R^3$. At the experimental radius $R \approx 80a$, the fundamental-mode (he$_{11}$) suppression factor is almost 10^{-5}, and indeed losses less than 1 dB/m (compared to the polymer loss of $\approx$50,000 dB/m) were observed experimentally.[37] This dramatic suppression of cladding/material losses is one reason why hollow-core fibers are potentially so important, because they lift the physical limitations imposed by available solid materials.

What is the source of this $1/R^3$ power law? The key fact is that the contribution to the loss from a particular absorbing material is proportional to the fraction of the electric-field energy in the material. One might jump to the conclusion that, for a core-guided mode (not a surface state), the losses will scale as $1/R$: if the field penetrates a certain distance d_p into the cladding, then the fraction of field in the cladding goes as the penetration area $2\pi R d_p$ divided by the core area πR^2, yielding $\sim 1/R$. Such an argument, however, assumes that the field *amplitude* $|\mathbf{E}|$ in the cladding compared to the core is independent of R, and in fact this is not the case. This is easiest to see for the te$_{01}$ mode, which by analogy with the metal waveguide has a node in $\mathbf{E}$ near $r = R$. As a consequence,[35] the te$_{01}$'s cladding $|\mathbf{E}|$ is proportional not to the field at $r = R$ (which is ≈ 0) but rather to the
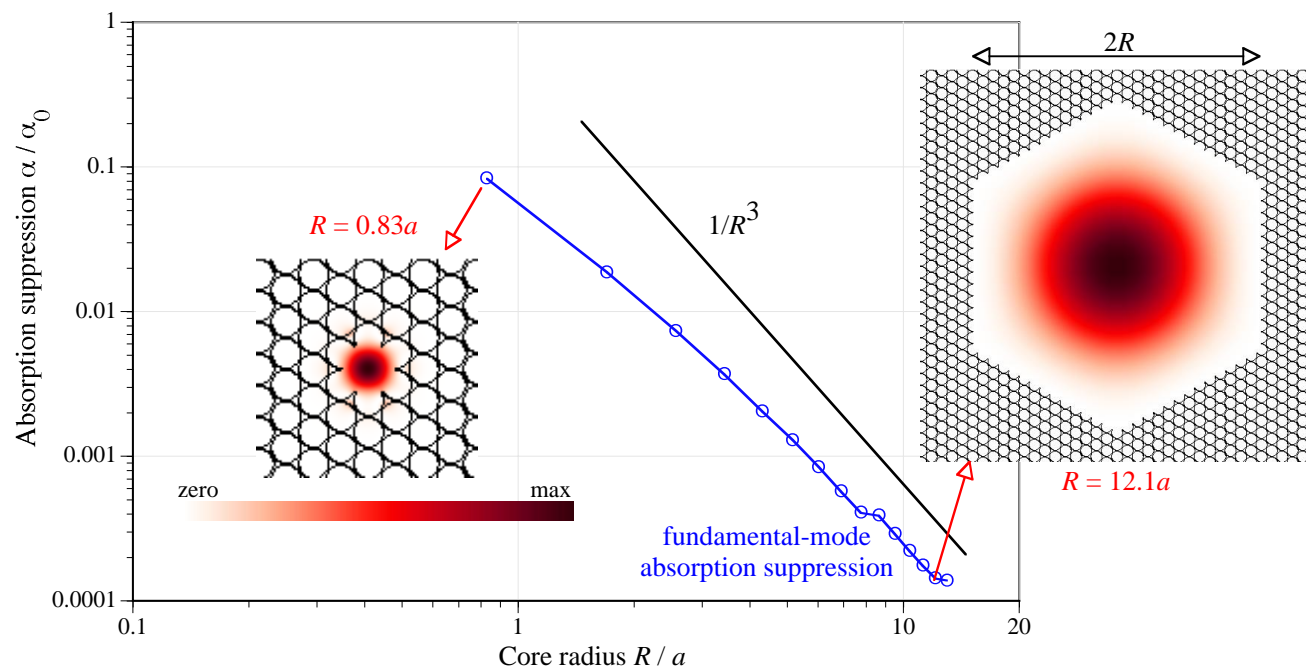
Figure 8. Scaling of the absorption suppression factor α/α_0 versus core radius R, at mid-gap, for the fundamental mode of a hollow-core holey fiber (blue circles/lines); this factor tends to a $1/R^3$ scaling (black line, for reference). Insets show the intensity pattern (time-average Poynting flux) of the fundamental mode for two core radii, $R = 0.83a$ and $R = 12.1a$. The dielectric interfaces are shown as black lines; the air core is hexagonal and terminates the crystal in such a way as to remove the possibility of surface states.[42]

slope $d|\mathbf{E}|/dr$ at $r = R$, which scales as $1/R$ for a fixed max $|\mathbf{E}|$ in the core. As a result, the te$_{01}$'s $|\mathbf{E}|^2$ in the cladding picks up an additional $1/R^2$ factor, and the absorption losses scale as $1/R^3$.

In fact, a similar argument holds for all core modes, because there is a variant on the scalar limit that holds as the core size is increased. (We did not appreciate this generalization in our earlier Ref. 35 publication.) For any given mode, in the limit of large R the mode becomes more and more similar to a plane wave propagating along the z axis. Its dispersion relation approaches the air light line, and its penetration depth into the cladding becomes negligible compared to the scale of the transverse oscillations. This condition, of the penetration into the inhomogeneous materials becoming small compared to the transverse wavelength $(2\pi/k_t)$, was precisely the condition in which the scalar limit applies. In this limit, we can describe the mode as a linear polarization multiplied by a scalar amplitude $\psi(x, y)$ that is zero in the cladding. In reality, there is some small nonzero amplitude in the cladding, but because of the approximate zero boundary condition at $r = R$, the amplitude of the cladding field goes as $1/R$ just as we explained for te$_{01}$. Thus, all modes approach a $1/R^3$ scaling.

What about two-dimensionally periodic photonic-crystal fibers, such as the hollow-core holey structure in Fig. 2(b)? Overall, the same asymptotic $1/R^3$ scaling should apply: the core interface/area ratio goes as $1/R$ and there is an additional $1/R^2$ factor from the cladding field amplitude in the scalar limit. However, an additional wrinkle is provided by the proliferation of surface state. Unless a crystal termination is chosen that eliminates surface states,[42–44] as the core size is increased we will get more and more surface states. These surface states cross the guided band and chop up its usable bandwidth.[42] Precisely such a phenomenon was observed experimentally when Ref. 45 replaced the air core of an earlier holey-fiber experiment by Ref. 46 with one of about 2.2 times the diameter: the losses were reduced by a factor of eight (from 13 dB/km to 1.6 dB/km), but the bandwidth was reduced by a factor of five because the surface states were not eliminated. (The surface states below the light line do *not* have absorption/leakage/scattering losses that decrease with R, because they remain localized at the cladding surface regardless of R.)

To see the $1/R^3$ scaling more convincingly in a holey fiber, however, one must look at a larger range of

core diameters, in a computer simulation where all other things can be kept rigorously equal (as opposed to two experiments by different groups that may or may not be comparable), and choose terminations so that the influence of surface states is eliminated. We have done so, looking at the fundamental air-guided mode of a hollow-core holey fiber in $\varepsilon = 2.1025$ silica with radius $0.47a$ air holes in a triangular lattice with period a, similar to Fig. 2(b). The core is a hexagonal-shaped air region carved out of the crystal with "radius" R, where $2R$ is the distance between two parallel sides of the hexagon. This structure, along with the intensity pattern of the fundamental mode, is shown for two sample core radii in the insets of Fig. 8. The core termination is chosen to roughly bisect a layer of holes, as in Ref. 42, to eliminate surface states. Then, we varied the core radius R (in steps of $a\sqrt{3}/2$ to preserve the termination) and computed the fraction of the fundamental mode's electric-field energy in the silica cladding material (equivalently, the absorption suppression factor) using a planewave-based eigensolver;[34] the fundamental mode was computed near mid-gap, at $\beta a/2\pi = 1.65$. The result is shown in Fig. 8, and indeed quickly approaches the expected $1/R^3$ asymptotic scaling.

4. CONCLUDING REMARKS

Although numerical computations will continue to be a central tool in the study of dielectric waveguides in general and photonic-crystal fibers in particular, the rare analytical theorems that rigorously constrain their properties are extremely valuable. To pick an extreme example, although one could perform numerical simulations of photonic crystals without knowing about conservation of energy or Bloch's theorem, the latter make the experiments much easier to design and the results much easier to interpret! While they are more modest in scope than Bloch's theorem or conservation laws, we hope that the results in this paper will provide new cornerstones of certainty to guide future understanding of these systems.

The results of the first half of this manuscript provide an absolute guarantee of index-guided modes under very broad circumstances; while it is true at every wavelength, it is especially illuminating in understanding the phenomenon of long-wavelength cutoffs, which can be very difficult to study numerically or experimentally as the modal diameter becomes large. The results of the second half highlight the importance of the scalar short-wavelength limit, which has many informative consequences even at moderate wavelengths, such as the origin of the gap or the scaling of the cladding losses with core radius.

ACKNOWLEDGMENTS

REFERENCES

1. J. D. Joannopoulos, R. D. Meade, and J. N. Winn, *Photonic Crystals: Molding the Flow of Light*, Princeton Univ. Press, 1995.
2. P. Russell, "Photonic crystal fibers," *Science* **299**(5605), pp. 358–362, 2003.
3. A. Bjarklev, J. Broeng, and A. S. Bjarklev, *Photonic Crystal Fibres*, Springer, New York, 2003.
4. F. Zolla, G. Renversez, A. Nicolet, B. Kuhlmey, S. Guenneau, and D. Felbacq, *Foundations of Photonic Crystal Fibres*, Imperial College Press, London, 2005.
5. A.-S. Bonnet-Bendhia and R. Djellouli, "High-frequency asymptotics of guided modes in optical fibres," *IMA J. Applied Math.* **52**(3), pp. 271–287, 1994.
6. T. A. Birks, J. C. Knight, and P. S. J. Russell, "Endlessly single-mode photonic crystal fiber," *Opt. Lett.* **22**(13), pp. 961–963, 1997.
7. R. Ramaswami and K. N. Sivarajan, *Optical Networks: A Practical Perspective*, Academic Press, London, 1998.
8. C. Elachi, "Waves in active and passive periodic structures: A review," *Proc. IEEE* **64**(12), pp. 1666–1698, 1976.
9. S. Fan, J. N. Winn, A. Devenyi, J. C. Chen, R. D. Meade, and J. D. Joannopoulos, "Guided and defect modes in periodic dielectric waveguides," *J. Opt. Soc. Am. B* **12**(7), pp. 1267–1272, 1995.

10. B. T. Kuhlmey, R. C. McPhedran, C. M. de Sterke, P. A. Robinson, G. Renversez, and D. Maystre, "Microstructured optical fibers: where's the edge?," *Opt. Express* **10**(22), pp. 1285–1290, 2002.

11. S. Kawakami and S. Nishida, "Characteristics of a doubly clad optical fiber with a low-index inner cladding," *IEEE J. Quantum Elec.* **10**(12), pp. 879–887, 1974.

12. T. Okoshi and K. Oyamoda, "Single-polarization single-mode optical fibre with refractive-index pits on both sides of core," *Electron. Lett.* **16**, pp. 712–713, 80.

13. W. Eickhoff, "Stress-induced single-polarization single-mode fiber," *Opt. Lett.* **7**(629–631), 1982.

14. J. R. Simpson, R. H. Stolen, F. M. Sears, W. Pleibel, J. B. Macchesney, and R. E. Howard, "A single-polarization fiber," *J. Lightwave Tech.* **1**(2), pp. 370–374, 1983.

15. M. J. Messerly, J. R. Onstott, and R. C. Mikkelson, "A broad-band single polarization optical fiber," *J. Lightwave Tech.* **9**(7), pp. 817–820, 1991.

16. H. Kubota, S. Kawanishi, S. Koyanagi, M. Tanaka, and S. Yamaguchi, "Absolutely single polarization photonic crystal fiber," *IEEE Photon. Tech. Lett.* **16**(1), pp. 182–184, 2004.

17. M.-J. Li, X. Chen, D. A. Nolan, G. E. Berkey, J. Wang, W. A. Wood, and L. A. Zenteno, "High bandwidth single polarization fiber with elliptical central air hole," *J. Lightwave Tech.* **23**(11), pp. 3454–3460, 2005.

18. P. Kuchment and B. Ong, "On guided waves in photonic crystal waveguides," *Waves in Periodic and Random Media, Contemporary Mathematics* **338**, pp. 105–115, 2004.

19. A. Bamberger and A. S. Bonnet, "Mathematical analysis of the guided modes of an optical fiber," *Journal on Mathematical Analysis* **21**(6), pp. 1487–1510, 1990.

20. H. P. Urbach, "Analysis of the domain integral operator for anisotropic dielectric waveguides," *Journal on Mathematical Analysis* **27**, 1996.

21. K. Yang and M. de Llano, "Simple variational proof that any two-dimensional potential well supports at least one bound state," *Am. J. Phys.* **57**(1), pp. 85–86, 1989.

22. B. Simon, "The bound state of weakly coupled Schrödinger operators in one and two dimensions," *Ann. Phys.* **97**(2), pp. 279–288, 1976.

23. E. N. Economou, *Green's functions in quantum physics*, Springer, 2006.

24. H. Picq, *Détermination et calcul numérique de la première valeur propre d'opérateurs de Schrödinger dans le plan.* PhD thesis, Université de Nice, Nice, France, 1982.

25. T. Inui, Y. Tanabe, and Y. Onodera, *Group Theory and Its Applications in Physics*, Springer, Heidelberg, 1996.

26. B. E. A. Saleh and M. C. Teich, *Fundamentals of Photonics*, Wiley, New York 1991.

27. D. R. Smith, D. C. Vier, T. Koschny, and C. M. Soukoulis, "Electromagnetic parameter retrieval from inhomogeneous materials," *Phys. Rev. E* **71**, p. 036617, 2005.

28. J. D. Jackson, *Classical Electrodynamics*, Wiley, New York, third ed., 1998.

29. A. W. Snyder and J. D. Love, *Optical Waveguide Theory*, Chapman and Hall, London, 1983.

30. A. Taflove and S. C. Hagness, *Computational Electrodynamics: The Finite-Difference Time-Domain Method*, Artech, Norwood, MA, 2000.

31. V. Kuzmiak, A. A. Maradudin, and F. Pincemin, "Photonic band structures of two-dimensional systems containing metallic components," *Phys. Rev. B* **50**, pp. 16835–16844, 1994.

32. A. Farjadpour, D. Roundy, A. Rodriguez, M. Ibanescu, P. Bermel, J. D. Joannopoulos, S. G. Johnson, and G. W. Burr, "Improving accuracy by subpixel smoothing in the finite-difference time domain," *Opt. Lett.* **31**, pp. 2972–2974, 2006.

33. D. Gloge, "Weakly guiding fibers," *Appl. Opt.* **10**(10), pp. 2252–2258, 1971.

34. S. G. Johnson and J. D. Joannopoulos, "Block-iterative frequency-domain methods for Maxwell's equations in a planewave basis," *Opt. Express* **8**(3), pp. 173–190, 2001.

35. S. G. Johnson, M. Ibanescu, M. Skorobogatiy, O. Weisberg, T. D. Engeness, M. Soljačić, S. A. Jacobs, J. D. Joannopoulos, and Y. Fink, "Low-loss asymptotically single-mode propagation in large-core OmniGuide fibers," *Opt. Express* **9**(13), pp. 748–779, 2001.

36. A. Argyros, T. A. Birks, S. G. Leon-Saval, C. M. B. Cordeiro, F. Luan, and P. S. J. Russell, "Photonic bandgap with an index step of one percent," *Opt. Express* **13**(1), pp. 309–314, 2005.

37. B. Temelkuran, S. D. Hart, G. Benoit, J. D. Joannopoulos, and Y. Fink, "Wavelength-scalable hollow optical fibres with large photonic bandgaps for CO_2 laser transmission," *Nature* **420**, pp. 650–653, 2002.

38. P. Roberts, F. Couny, H. Sabert, B. Mangan, D. Williams, L. Farr, M. Mason, A. Tomlinson, T. Birks, J. Knight, and P. S. J. Russell, "Ultimate low loss of hollow-core photonic crystal fibres," *Opt. Express* **13**(1), pp. 236–244, 2005.

39. W. D. Warters, "WT4 millimeter waveguide system: introduction," *Bell Syst. Tech. J.* **56**, pp. 1825–1827, 1977. The introduction to a special issue with many useful articles.

40. W. H. Weber, S. L. McCarthy, and G. W. Ford, "Perturbation theory applied to gain or loss in an optical waveguide," *Appl. Opt.* **13**(4), pp. 715–716, 1974.

41. S. G. Johnson, M. L. Povinelli, M. Soljačić, A. Karalis, S. Jacobs, and J. D. Joannopoulos, "Roughness losses and volume-current methods in photonic-crystal waveguides," *Appl. Phys. B* **81**, pp. 283–293, 2005.

42. J. West, C. Smith, N. Borrelli, D. Allan, , and K. Koch, "Surface modes in air-core photonic band-gap fibers," *Opt. Express* **12**(8), pp. 1485–1496, 2004.

43. K. Saitoh, N. A. Mortensen, and M. Koshiba, "Air-core photonic band-gap fibers: the impact of surface modes," *Opt. Express* **12**(3), pp. 394–400, 2004.

44. H. K. Kim, M. J. F. Digonnet, G. S. Kino, J. Shin, and S. Fan, "Simulations of the effect of the core ring on surface and air-core modes in photonic bandgap fibers," *Opt. Express* **12**(15), pp. 3436–3442, 2004.

45. B. J. Mangan, L. Farr, A. Langford, P. J. Roberts, D. P. Williams, F. Couny, M. Lawman, M. Mason, S. Coupland, R. Flea, and H. Sabert, "Low loss (1.7 db/km) hollow core photonic bandgap fiber," in *Proc. Opt. Fiber Commun. (OFC).*, Optical Society of America, (Los Angeles), 2004. Paper PDP24.

46. C. M. Smith, N. Venkataraman, M. T. Gallagher, D. Müller, J. A. West, N. F. Borrelli, D. C. Allan, and K. W. Koch, "Low-loss hollow-core silica/air photonic bandgap fibre," *Nature* **424**, pp. 657–659, 2003.